Chemistry & Biology, Vol. 12, 1085–1091, October, 2005, ©2005 Elsevier Ltd All rights reserved. DOI 10.1016/j.chembiol.2005.07.010

Supramolecular Fluorophores for Biological Studies: Phenylene Vinylene-Amino Acid Amphiphiles

Daniel A. Harrington,[1] Heather A. Behanna,[2] Gregory N. Tew,[2,4] Randal C. Claussen,[2] and Samuel I. Stupp[1,2,3,*]
[1]Department of Materials Science and Engineering
[2]Department of Chemistry
[3]Feinberg School of Medicine
Northwestern University
Evanston, Illinois 60208-3108

Summary

We report here on a family of self-assembling fluorescent organic amphiphiles with a biomolecular L-lysine hydrophile and a photonically active phenylene vinylene hydrophobe. Unlike conventional amphiphiles, these segmented dendrimers feature a rigid, branched hydrophobe, and have packing characteristics controlled by the ratio of cross-sectional areas of the hydrophobe and hydrophile. In dilute solution, the amphiphiles form supramolecular aggregates, which are easily taken in by cells through an endocytic pathway, and have no discernible effect on cell proliferation or morphology. An analogous pyrene-based amphiphile was cytotoxic, suggesting that cell survival may be linked either to the self-assembling nature of the amphiphiles, or to the specific properties of the phenylene vinylene segment. The combination of photonic and biological components in these amphiphiles provides great potential for applications in sensing or delivery of molecules to intracellular targets.

Introduction

Amphiphilic systems play a key role in both structure and function in cellular biology. Their unique structural and chemical properties enable self-organization in aqueous environments into a variety of shapes, over many length scales. Discrete cellular compartmentalization by lipid bilayers and tertiary protein structures relies heavily on the self-assembly of amphiphiles. Thus, the importance of biological amphiphiles continues to inspire research on synthetic molecules that contain discrete hydrophilic and hydrophobic segments [1–5]. As in nature, synthetic amphiphiles have been found to organize into a wide variety of structures, including cylinders, lamellae, micelles, and vesicles [6–10]. We report here on a distinct class of amphiphilic structures based on segmented dendrimers that contain phenylene vinylene (PV) and L-lysine structural units. These molecules self-assemble into nanoscale aggregates in aqueous solution and accumulate within discrete compartments of multiple cell lines, with no discernible effect on cell proliferation or morphology. These nanomaterials could be useful to probe biological systems, track the delivery of therapeutic cargo to subcellular structures, or study biochemical pathways.

The molecular architectures used in this work are inspired by earlier work from Hawker and Fréchet [11] and others [12–16] who reported on segmented dendrimers. In their original work, the two segments, aryl ethers and aryl esters, were chemically very similar, and, in fact, no phase separation was observed in mixtures of the pure dendrimers. (When homopolymers of aryl ether and aryl ester dendrimers were mixed, a single DSC transition was observed, suggesting no phase separation between the two different systems.) This concept was revisited in later work by Gillies and Fréchet [17], in which amphiphilic "bow-tie" molecules were constructed by attaching oligomeric chains of poly(ethylene oxide) to polyester dendrons. Other dendrimeric amphiphiles, containing flexible alkyl tails and free amines, were described by Joester et al. for gene delivery applications [5]. In our work reported here, the two blocks, L-lysine and phenylene vinylene, are both dendrimeric and are coupled after separate syntheses. The hydrophobic PV segment of the amphiphile is known as a rigid moiety that can drive molecular self-assembly [18–21]. Multiple generations of PV can be constructed by orthogonal application of the Horner-Wadsworth-Emmons and Heck reactions [22]. All generations of PV fluoresce under ultraviolet illumination, and thus these molecules can be used as fluorescent probes, which are compatible with 4′,6-diamidino-2-phenylindole (DAPI)-type filters. In addition, dendritic PV can be functionalized with a variety of groups to modify its electronic properties or to provide binding domains for sensing applications. Multiple generations of the hydrophilic amino acid segment can be developed through standard solution-phase coupling and deprotection of the α and ε amino groups on L-lysine [23, 24]. This segment provides a hydrophilic portion for the molecule and is designed for subsequent incorporation of more complex peptidic segments to direct recognition in biological systems. Various generations of the PV (Gx^{PV}) and the L-lysine (Gx^{lys}) are then connected via a β-alanine linker (Figure 1). The resultant Gx^{PV}-Gx^{lys} amphiphiles presented here are structurally interesting due to their conformationally rigid hydrophobe, which results in a large ratio of the hydrophobe: hydrophile cross-sectional area (unlike most well-known surfactants) [25–30]. These characteristics were expected to induce aggregation of the molecules in aqueous media, as described below.

Functionally, it seemed clear that these molecules could potentially be used in a variety of biological applications. There are few reports of cell interactions with stilbene-type molecules, and most involve natural derivatives that are much more highly functionalized than the molecules presented in Figure 1 [31–33]. The PV dendron segment, if well-tolerated by cells, could be easily modified in future applications to modulate its range of excitation/emission, or to attach binding sites for ions or other small signaling molecules. We also anticipated

*Correspondence: s-stupp@northwestern.edu
[4]Present address: Department of Polymer Science and Engineering, University of Massachusetts, Amherst, Massachusetts 01003.

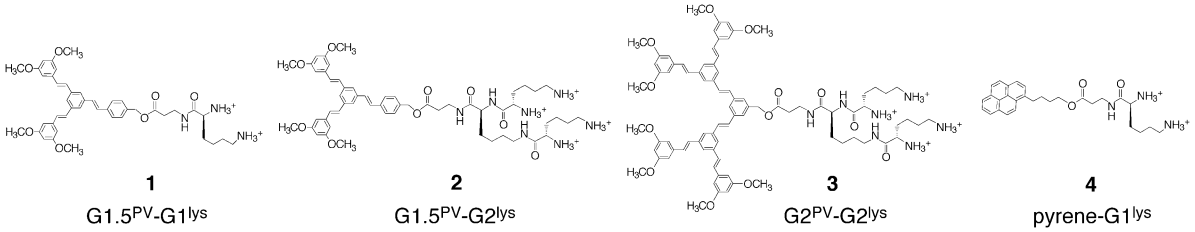

Figure 1. Structures of Phenylene Vinylene-L-Lysine Segmented Dendrimers

4 was synthesized as a fluorescent analog to **1**.

that the L-lysine segment of these molecules could potentially bind plasmids, growth factor surfaces, or other biosignals. Here, we report on our initial in vitro explorations with these molecules to assess their cytotoxicity, identify their interaction with cells, and evaluate the fluorophore's resistance to degradation in a biological environment.

Results and Discussion

^{1}H nuclear magnetic resonance (NMR) of the family of amphiphiles **1–3** is shown in Figure 2. In deuterium oxide (D_2O), a broadening of peaks was observed in the aromatic region, while upfield peaks were still well resolved. In solvents such as d_6-dimethylsulfoxide (d_6-DMSO), a good solvent for both segments, these same aromatic peaks were better resolved. In addition to signal broadening, we also observed a large upfield shift in the aromatic protons, which is consistent with aromatic-aromatic interactions [34]. This suggested that molecules **1–3** self-assemble in dilute aqueous solution, with the L-lysine groups exposed to the aqueous environment, while the nonpolar PV segments are buried in the interior of the aggregate. Furthermore, the extent of aromatic broadening in NMR appeared to be dependent on the comparative generation sizes of the hydrophobe and the hydrophile, i.e., **1** and **3** broadened and shifted more significantly than **2**.

Fluorescence emission and excitation spectra were then collected for **1–3** in water (Figure 3). As concentration increased, all three molecules showed a red shift in their excitation spectra, characteristic of J-aggregate formation [35]. This observation confirmed the indications of close fluorophore interaction seen by NMR. For **1** and **3**, the gradual, concentration-dependent excitation shift began at concentrations above 8×10^{-6} M, with a maximum observed shift of more than 60 nm. In contrast, the red shift for **2** occurred only above 6×10^{-5} M. This order of magnitude difference also reflected the aggregation trends observed by NMR, with **1** and **3** demonstrating notably different aggregation behavior than **2**.

Supramolecular self-assembly in dilute aqueous solution was explored further by dynamic light scattering (DLS). Multiple populations of structures were observed for of all the molecules, with a linear dependence of the aggregate size on concentration. For **1** and **3**, which have equal generation size of hydrophobic and hydrophilic segments, small aggregates ranging in size from 10 to 20 nm accounted for ca. 5% of the total population. However, the majority of observed structures ranged in size from 80 to 120 nm for **1**, and from 20 to 40 nm for **3**. In contrast, aqueous suspensions of **2** produced much smaller nanostructures than **1** and **3**, and the majority of populations were 5–10 nm, and only a small percentage of structures ranged from 15 to 30 nm. Interestingly, **2** did not give a DLS signal below 1.2×10^{-3} M, while aggregates were observed for **1** and **3** at dilutions as low as 4×10^{-6} M. With this initial data for amphiphile assembly in deionized (DI) water, we proceeded to examine the aggregation of **1** and **2** in standard cell culture media. Because of their better solubility in aqueous solution, and initial observations of faster cell uptake (described below), **1** and **2** were selected for further in vitro work. By DLS in Dulbecco's modified Eagle's media (DMEM), **2** showed minimal difference in its aggregate formation, while **1** shifted to a monomodal distribution of particles that were 30 nm in size. Ionic effects are well-known in influencing amphiphile assembly, and the substantial shift in behavior for **1** indicated that the larger populations observed in DI water might be composed of smaller primary particles. Amphiphiles **1** and **2** were therefore examined in the dried state by using transmission electron microscopy

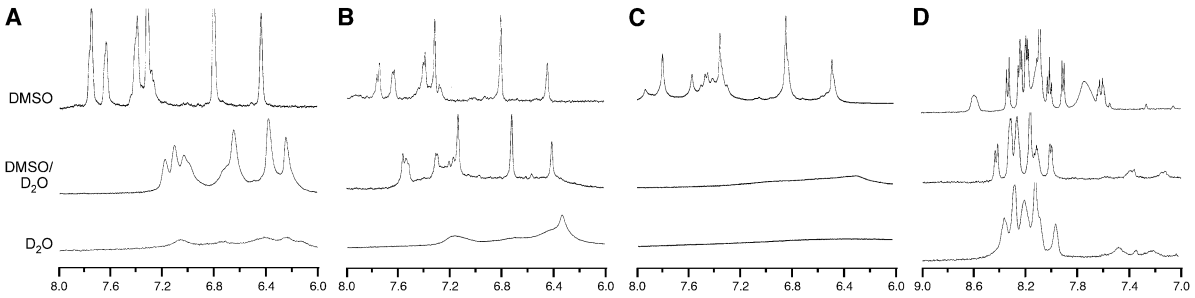

Figure 2. ^{1}H NMR of Self-Assembling Molecules at 10^{-3} M in d_6-DMSO, 50/50 d_6-DMSO, and D_2O

(A–D) X axis units are measured in ppm. (A) **1**. (B) **2**. (C) **3**. (D) **4**.

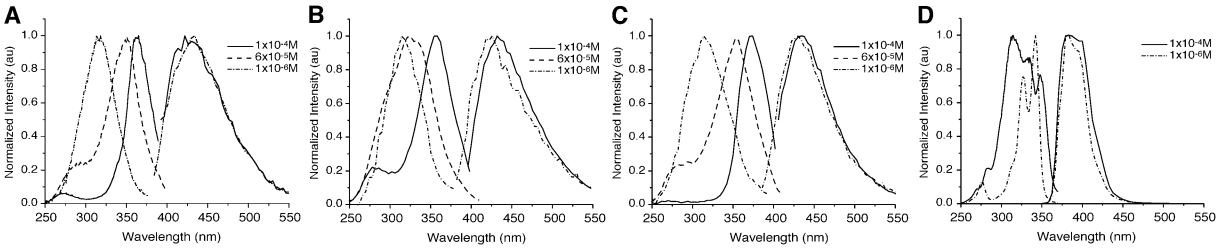

Figure 3. Excitation/Emission Spectra for **1**, **2**, **3**, and **4**

(A–D) **1** is shown in (A), **2** is shown in (B), **3** is shown in (C), and **4** is shown in (D). Excitation scans for (A)–(C) were collected with emission held constant at λ_{em} = 434 nm. Emission spectra were collected at λ_{ex} = 314 and 370 nm. A concentration-dependent red shift in excitation maximum was seen for all three Gx^{PV}-Gx^{lys} systems. A scan at 6 × 10^{-5} M indicates that the shift began earlier for **1** and **3** than for **2** as concentration was increased.

(TEM), in an effort to visualize particle morphology (Figure S3; see the Supplemental Data available with this article online). Images of both amphiphiles showed small primary particles, 5–10 nm in diameter, which were closely associated with each other, suggesting that the bimodal distributions observed by DLS may represent an equilibrium between primary particles and larger secondary aggregates. Notably, this information was obtained in the dried state, with the associated potential artifacts that this includes. Cryo-TEM or -SEM methods would undoubtedly provide more detailed information regarding aggregate distribution in situ.

We also evaluated the lysine hydrophiles on the periphery of the aggregates via a pH titration of the amphiphiles in aqueous solution (Figure 4). Aggregation has been previously shown to affect protonation behavior, and we expected that these molecules might demonstrate a similar response. As shown in Figure 4, unmodified L-lysine demonstrates relatively sharp transitions. These features broadened and shifted as molecules with a methyl group and a G1 PV segment were titrated from pH 11 to 4. Even further shifts were observed for **2**, with its second-generation lysine segment. This behavior has been observed previously by others for

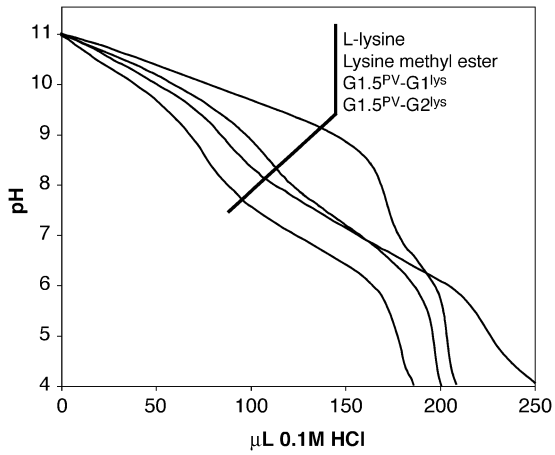

Figure 4. pH Titration of L-Lysine Derivatives in Aqueous Solution

Solutions of each molecule at equivalent amine concentrations were incrementally titrated with 0.1 M HCl. As more complex hydrophobes were covalently coupled to L-lysine, the molecules' transitions broadened and shifted, indicating a change in protonation behavior.

full lysine dendrimers [36], and has been attributed to the close interactions of terminal lysines, which each influence the protonation of other neighboring amines. That this was observed for noncovalent interactions within a self-assembling system is consistent with the close association of amines on the periphery of assembled objects.

These observations of self-assembly behavior demonstrate that the ratio of hydrophobe:hydrophile cross-sectional area strongly influences the formation of supramolecular structures. When this ratio is increased in the Gx^{PV}-Gx^{lys} systems, larger aggregates are observed that persist to a much higher dilution. We believe that these larger aggregates result from an inability of the molecularly rigid hydrophobes to pack efficiently into the interior of a small spherical micelle. As a result, amphiphiles **1** and **3** default to larger, less frustrated structures. In contrast, amphiphile **2** has a lower ratio of hydrophobe:hydrophile cross-sectional area, which then directs the system toward small micelle formation, despite its rigid hydrophobe. This packing is also expected to influence the interactions among lysines on the periphery of a primary aggregate. While terminal amines on L-lysine are largely protonated at neutral pH, the same cannot be said for a lysine-decorated aggregate. The covalently coupled hydrophobe appears to influence the interaction of the hydrophiles, which could then alter the surface charge or hydrogen bonding on that particle's surface, and enable the formation of larger aggregates-of-aggregates. This tuning seems to be largely controlled by the relative ratio of cross-sectional area between the hydrophobe and hydrophile. Surprisingly, the lower limit for aggregation of **2** observed by DLS was 1.2 × 10^{-3} M, while aggregates were observed by fluorescence down to 6 × 10^{-5} M. This observation is repeatable, but it is still not easily explained. We expect that the difference might also correlate with the relatively larger hydrophile in **2** as compared to **1** and **3**.

To examine the interaction of these amphiphiles with biological systems, two separate cell types, Swiss Albino 3T3 mouse embryo fibroblasts and primary bovine chondrocytes, were exposed to thin films of **1**, **2**, and **3** in vitro. Through gradual dissolution into the media, the amphiphiles were taken up by cells in a concentration-dependent manner, and they were observed to localize within the cytosol in discrete spherical compartments (Figure 5). The fluorescent molecules were

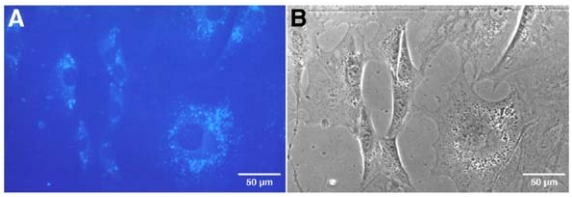

Figure 5. 3T3 Fibroblasts on a Glass Surface after 24 hr of Exposure to **1**

(A) Fluorescence image using a DAPI filter set.
(B) Phase contrast image of the same area as shown in (A).

typically visible in cells within 4 hr of exposure (depending on the molecule and concentration), and they remained noncytotoxic at routine working concentrations (<10 μM) for several days (Figure S4). Notably, neither $G1.5^{PV}$ nor $G2^{PV}$ alone were observed within cells after several days of exposure; thus, the covalent attachment of Gx^{lys} to form the amphiphile is a requirement for cell uptake. Figure 5 is a representative example of fibroblast cells after exposure to **1**, **2**, or **3**. The image in Figure 5A shows emission from **1**, which has been internalized and confined in discreet spherical structures within the cell cytosol; Figure 5B is a phase contrast image of the same area. The size, shape, and number of intracellular structures containing **1** suggested to us that the fluorescent amphiphile was either being stored or trafficked to specific organelles. To examine this, cells were pre-exposed to **1** and costained with markers for cell organelles. Mitochondria stained with a commercial fluorescent dye (Figure 6A) appeared diffuse and irregular throughout each cell, with little resemblance to the staining pattern of the Gx^{PV}-Gx^{lys}-containing structures. Immunochemical staining of lysosomes (Figure 6B), however, identified a staining pattern within the cells with very similar structural shape, size, and population to that of **1**, **2**, and **3**. Calculations on multiple samples indicated an average colocalization of these structures of at least 44%. This suggests that the amphiphiles are taken into cells from the media through an endocytic pathway, with eventual accumulation in lysosomes. Notably, the phenylene vinylene segment of the amphiphiles could withstand the typical acidic conditions and proteolytic enzymes in a lysosome without a substantial loss of fluorescence.

A qualitative difference in the rate of cell uptake of the Gx^{PV}-Gx^{lys} molecules was observed throughout the course of these experiments, and this uptake followed the order $G1.5^{PV}$-$G2^{lys}$ > $G1.5^{PV}$-$G1^{lys}$ >> $G2^{PV}$-$G2^{lys}$. This order of uptake again correlates with the size of the hydrophilic segment, as well as with the size ratio between the hydrophobe and the hydrophile. In an effort to better quantify this difference, 3T3 fibroblasts were plated onto 24-well plates and incubated with the amphiphiles in the cell media. At various time points, the wells were aspirated, rinsed, and scanned on a fluorescence plate reader to identify the amount of amphiphile within each well (i.e., the amount of amphiphile retained by the cells). As shown in Figure 7, the averaged intensity values for **2** were approximately double of those recorded for **1**. To further test cell uptake via endocytosis, both of these amphiphiles were also tested on cells incubated at 4°C, a temperature at which

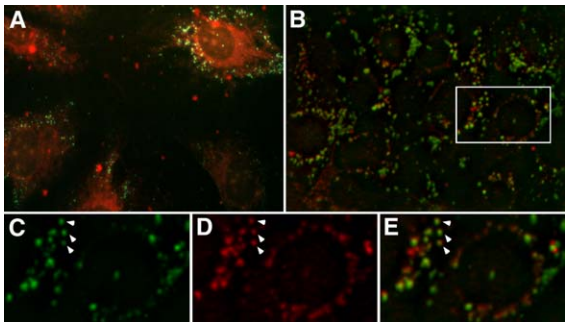

Figure 6. Colocalization Images for 3T3 Fibroblasts Preexposed to **1**

(A) Cells costained for **1** (blue) and mitochondria (red), demonstrating dissimilar staining patterns.
(B) Cells costained for **1** (false green) and lysosomes (red), demonstrating consistent overlap (yellow) and morphology.
(C–E) Green, red, and overlay channels, respectively, of inset region.

endocytic processes are halted. Uptake of both materials was greatly reduced, to near-baseline values, under these conditions. Cells incubated with **3** (data not shown) did not yield a sufficiently strong signal for detection by the plate reader, but the molecule uptake was confirmed visually via fluorescence microscopy. Notably, we used all molecules at standard working concentrations for fluorophores (<10 μM), which were eventually below the aggregated state. However, molecules **1–3** all demonstrated qualitatively similar cell uptake at both aggregating and nonaggregating concentrations.

To further explore cell interaction with these amphiphiles, we synthesized **4** (Figure 1), a pyrene analog, to determine if a similarly rigid, hydrophobic fluorophore could replace the PV. When fibroblasts were exposed to thin films of **4**, the molecule was taken up by the cells (although not within specific compartments), and nearly all of the cells died (Figure S5). Cells that were incubated

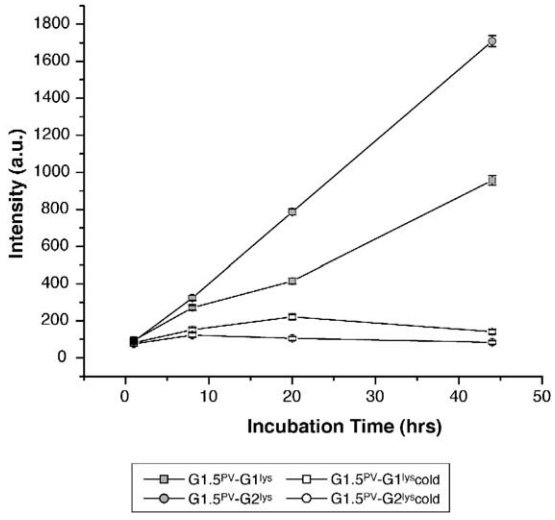

Figure 7. Fibroblast Uptake of **1** and **2** over Time

Fluorophore uptake increased over time for cells in normal culture conditions. Exposure to **4** (not shown) resulted in complete cell death and no recordable signal. Error bars indicate the standard error of the weighted mean.

with **4** for the plate reader experiment in Figure 7 all died by the first time point, and they were not retained on the plate surface after rinsing. Interestingly, this pyrene-based molecule has different aggregation behavior than the Gx^{PV}-Gx^{lys} series. For example, aromatic peaks in the NMR broadened slightly in water but did not disappear or shift upfield (Figure 2D). Also, aggregates were only observed by DLS at concentrations above 5×10^{-4} M, and no concentration-dependent phenomena, such as a red shift or excimer formation, were observed in the excitation/emission spectra (Figure 3D). Pyrene derivatives are well-known to solubilize in lipid bilayers, and **4** did not demonstrate evidence of a closely associated aggregate structure. In contrast, **1**, **2**, and **3** were easily taken in by cells, with no substantial indication of cytotoxicity.

We are currently investigating the mechanisms through which these segmented dendrimers accumulate within cells and are attempting to understand in greater detail the large difference in toxicity observed among the amphiphiles. While substantial differences in self-assembly properties were observed between the PV-based and the pyrene-based molecules, it is also possible that cytotoxicity for both types of systems is mediated on the molecular level, rather than at the aggregate level. For all of the molecules, however, the addition of the hydrophilic segment was responsible for enabling the uptake of the fluorophore. It is notable that in their aggregated state, the Gx^{PV}-Gx^{lys} molecules present a peripheral poly-lysine surface, and their facile uptake is reminiscent of that seen for other peptides, such as poly-arginine and Tat domain conjugates [37, 38]. It is likely that the cationic nature of the Gx^{PV}-Gx^{lys} surface is what mediates their endocytosis. From these experiments, it appears clear that the self-assembling properties of the Gx^{PV}-Gx^{lys} molecules, as well as the unusual nature of the PV hydrophobe, strongly influence the molecules' interactions with cells and moderate any potential cytotoxicity.

Significance

A class of fluorescent amphiphiles based on segmented dendrimers that forms nanostructures in aqueous solutions is reported. The aggregation of these molecules is controlled by the ratio of the cross-sectional area between the rigid hydrophobe and the hydrophile, which directed the amphiphiles to pack into one or more levels of supramolecular structures. This contrasts the behavior of most common surfactants, in which tapered molecular geometries lead instead to the formation of spherical micelles [25]. The uncommon rigidity of the PV hydrophobe, and its influence on aggregate size and stability, may also be responsible for the observed biological behavior. The segmented dendrimer materials all collect in discreet compartments within the endocytic pathway of living mammalian cells, with no significant cytotoxicity, and retain their photoluminescent behavior. In contrast, a similar amphiphile with a pyrene fluorophore had high cytotoxicity. Both segments of the Gx^{PV}-Gx^{lys} molecules offer flexible chemistries that could be individually modified in the future to include a ratiometric fluorophore or a peptidic segment with greater specificity for cellular targets. For this reason, we envision their potential use in biosensing, labeling organelles, or tracking the delivery of molecules to cellular targets.

Experimental Procedures

Synthesis and Characterization

All synthetic reagents were purchased from Sigma-Aldrich. Amphiphiles **1**–**3** were constructed by synthesizing multiple generations of phenylene vinylene and L-lysine separately, and coupling these in methylene chloride, a mutually compatible solvent. The synthesis of each segment has been reported previously and is described in detail in the Supplemental Data. Multiple generations of the hydrophilic amino acid segment were developed through standard solution-phase coupling and deprotection of the α and ε amino groups on L-lysine. Multiple generations of PV were constructed by orthogonal application of the Horner-Wadsworth-Emmons and Heck reactions [22]. Molecule **9** (Figure S1) is considered a first-generation "G1" dendrimer. Molecule **11** was developed for easier coupling to L-lysine dendrons and is identified as "G1.5" due to the additional PV segment required for this coupling. Molecule **4** was synthesized through similar carbodiimide coupling of 1-pyrenebutanol to Boc-protected L-lysine with subsequent deprotection. NMR studies were performed on a 500 MHz Varian Inova spectrometer, by using the concentrations and solvents listed. DLS studies were performed on a Brookhaven BI-9000 digital correlator, by using a 514 nm laser set at a 90° geometry. Amphiphiles were ultrasonicated in purified water (18.2 MΩ·cm resistivity, from a Millipore filtration system) for 10 min prior to DLS analysis and were filtered though 0.45 μm pore size poly(tetrafluoroethylene) syringe filters immediately before data collection. Ten collections were performed for each sample and were analyzed by using the nonnegatively constrained least-squares (NNLS) fit from the Brookhaven 9KDLSW software, and Microcal Origin software for additional curve fitting. Fluorescence studies were conducted on an ISS PC1 steady-state fluorescence spectrometer. Samples were prepared for TEM imaging by drop casting from dilute aqueous solution onto a holey carbon-coated TEM grid, and excess liquid was wicked away. Grids were then stained with 2% phosphotungstic acid to enhance contrast. pH titrations were performed with each amphiphile at 7.6 mM concentration of amino groups, in 0.1 M KCl. The solution pH for each sample was increased gradually to pH 11; then, solutions were titrated with 1–3 μl additions of 0.1 M HCl to reach pH 4. Solutions were allowed to equilibrate between additions before the pH change was recorded.

Cell Culture Experiments

All cell media supplies were obtained from GIBCO/Invitrogen, unless otherwise specified. Cell culture studies were conducted by exposing cells to the amphiphile either as a solid film, or by adding it directly to the cell media in methanol. For thin film studies, 10 μl amphiphile, dissolved at 10 mg/ml in methanol, was placed onto two opposite corners of a 2-well glass chamber slide (Nalge Nunc), and the patches were allowed to dry. 3T3 Swiss Albino mouse embryo fibroblasts (CCL-92, American Type Culture Collection) were cultured in DMEM + 10% FBS (Hyclone Laboratories) + 1% penicillin/streptomycin to near-confluence, trypsinized, and plated in the treated chamber slides at 2×10^4 cells/well. After 24 hr of incubation at 37°C/10% CO_2, cell images were captured with a Nikon TE200 microscope and epifluorescence source, with a standard DAPI filter cube.

For proliferation studies, 3T3 fibroblasts were plated on 12-well tissue culture-treated polystyrene (TCPS) plates (Corning) at 1×10^4 cells/well and were allowed to attach overnight, by using media and culture conditions as described above. Molecule **1** was dissolved in methanol and added directly to the cell media at 5 μl per 2 ml of media. At each time point, cells were trypsinized, resuspended in serum-containing media and trypan blue, and counted with a hemocytometer. Each well was counted four times, and each condition was repeated in triplicate. Statistical calculations were performed by using the ANOVA plug-in in Microsoft Excel software.

For colocalization studies, fibroblasts were grown in chamber slides and pre-exposed to **1** by either the solid-film or solution-phase methods described above. Mitochondrial staining was then achieved by incubating cells in media containing 500 nM Mito-Tracker Red CMXRos (Molecular Probes) for 30 min. Mitochondria-stained samples were rinsed with Hank's buffered salt solution (with calcium and magnesium), fixed with 10% neutral buffered formalin for 5 min, and mounted for visualization. To stain lysosomes, cells were pre-exposed to **1** and then fixed for 5 min in neutral buffered formalin. Following standard immunochemistry protocols, cells were permeabilized and incubated with antibodies to either LAMP-1 or LAMP-2 lysosomal membrane proteins (1D4B and ABL-93, respectively). These antibodies, developed by Thomas August, were obtained from the Developmental Studies Hybridoma Bank, under the auspices of the National Institute of Child Health and Human Development, and were maintained by the University of Iowa, Department of Biological Sciences. Secondary antibodies coupled to the tetramethylrhodamineisothiocyanate (TRITC) fluorophore were used for visualization (Sigma-Aldrich). Fluorescence images in a z-series from lysosome experiments were deconvolved with iterative restoration, and the colocalization of fluorescent structures was quantified and rendered, by using Improvision Volocity software.

For plate reader experiments, 3T3 fibroblasts were grown to near confluence, trypsinized, plated into 24-well TCPS plates, and incubated overnight. Fluorescent amphiphiles were solubilized in methanol, and 5 μl was added to the 1 ml of media in each well, yielding a final concentration of 50 μM. The plates were incubated for 1, 8, 20, and 44 hr, either in standard incubation conditions, or were sealed and stored at 4ºC. Media were aspirated from each well, and the cell surface was gently rinsed with 200 μl HBSS (with calcium and magnesium). The HBSS was aspirated and replaced with 300 μl HBSS, and plates were immediately scanned in a Molecular Devices Gemini EM fluorescence plate reader, in bottom read mode. Each well scan was conducted as a 5 × 5 array, with seven scans per point, at 360/425 ex/em. The SoftMax plate reader software was used to obtain the average and standard deviation of the 21 measurements taken across each well. The duplicate wells for each condition were then averaged by using a weighted mean and weighted error.

Supplemental Data

Supplemental Data including synthetic details, TEM micrographs of the amphiphiles, and additional data regarding cell behavior are available at http://www.chembiol.com/cgi/content/full/12/9/1085/DC1/.

Acknowledgments

This work was supported by a grant from the U.S. Army Research Office (DAAH04-96-1-0450), the Department of Energy (DE-FG02-00ER45810), the National Science Foundation (EEC-0118025/001), and the National Institutes of Health (R01 EB003806-01). D.A.H. was supported by a Walter P. Murphy fellowship. The authors would like to acknowledge Julia Hwang for her contributions to initial cell studies, and Jeff Hartgerink for TEM imaging of the amphiphiles. The authors also acknowledge the use of the Biological Imaging Facility, the Keck Biophysics Facility, and the Electron Probe Instrumentation Center at Northwestern University.

Received: May 12, 2005
Revised: July 19, 2005
Accepted: July 26, 2005
Published: October 21, 2005

References

1. Ariga, K., Urakawa, T., Michiue, A., Sasaki, Y., and Kikuchi, J. (2000). Dendritic amphiphiles: dendrimers having an amphiphile structure in each unit. Langmuir *16*, 9147–9150.
2. Escuder, B., Rowan, A.E., Feiters, M.C., and Nolte, R.J.M. (2001). Aggregation behaviour and binding properties of an L-lysine appended glycoluril receptor. Tetrahedron Lett. *42*, 2751–2753.
3. Menger, F.M., and Marappan, S. (2000). Synthesis and properties of a poly-bolyte. Langmuir *16*, 6763–6765.
4. Raudino, A., Cantu, L., Corti, M., and Del Favero, E. (2000). Bistable molecular self assembling. Curr. Opin. Colloid In. Sci. *5*, 13–18.
5. Joester, D., Losson, M., Pugin, R., Heinzelmann, H., Walter, E., Merkle, H., and Diederich, F. (2003). Amphiphilic dendrimers: novel self-assembling vectors for efficient gene delivery. Angew. Chem. Int. Ed. Engl. *42*, 1486–1490.
6. Mueller, A., and O'Brien, D.F. (2002). Supramolecular materials via polymerization of mesophases of hydrated amphiphiles. Chem. Rev. *102*, 727–758.
7. Hartgerink, J.D., Zubarev, E.R., and Stupp, S.I. (2001). Supramolecular one-dimensional objects. Curr. Opin. Solid St. Mat. Sci. *5*, 355–361.
8. Lehn, J.-M. (1995). Supramolecular Chemistry (New York: VCH).
9. Sone, E.D., Zubarev, E.R., and Stupp, S.I. (2002). Semiconductor nanohelices templated by supramolecular ribbons. Angew. Chem. Int. Ed. Engl. *41*, 1705–1709.
10. Arnt, L., and Tew, G.N. (2002). New poly(phenyleneethynylene)s with cationic, facially amphiphilic structures. J. Am. Chem. Soc. *124*, 7664–7665.
11. Hawker, C.J., and Fréchet, J.M. (1992). Unusual macromolecular architectures - the convergent growth approach to dendritic polyesters and novel block copolymers. J. Am. Chem. Soc. *114*, 8405–8413.
12. Chow, H.F., and Mak, C.C. (1997). Preparation and structure-chiroptical relationships of tartaric acid-based layer-block chiral dendrimers. J. Chem. Soc., Perkin Trans. 1 *2*, 91–95.
13. Gudat, D. (1997). Inorganic cauliflower: functional main group element dendrimers constructed from phosphorous- and silicon-based building blocks. Angew. Chem. Int. Ed. Engl. *36*, 1951–1955.
14. Maraval, V., Laurent, R., Donnadieu, B., Mauzac, M., Caminade, A.M., and Majoral, J.P. (2000). Rapid synthesis of phosphorus-containing dendrimers with controlled molecular architectures: First example of surface-block, layer-block, and segment-block dendrimers issued from the same dendron. J. Am. Chem. Soc. *122*, 2499–2511.
15. Trollsås, M., Claesson, H., Atthoff, B., and Hedrick, J.L. (1998). Layered dendritic block copolymers. Angew. Chem. Int. Ed. Engl. *37*, 3132–3136.
16. Maraval, V., Sebastian, R.M., Ben, F., Laurent, R., Caminade, A.M., and Majoral, J.P. (2001). Varying topology of dendrimers - a new approach toward the synthesis of di-block dendrimers. Eur. J. Inorg. Chem. *7*, 1681–1691.
17. Gillies, E., and Frechet, J.M.J. (2002). Designing macromolecules for therapeutic applications: polyester dendrimer-poly(ethylene oxide) "bow-tie" hybrids with tunable molecular weight and architecture. J. Am. Chem. Soc. *124*, 14137–14146.
18. Tew, G.N., Li, L.M., and Stupp, S.I. (1998). Polar and luminescent supramolecular films. J. Am. Chem. Soc. *120*, 5601–5602.
19. Tew, G.N., Pralle, M.U., and Stupp, S.I. (1999). Supramolecular materials from triblock rodcoil molecules containing phenylene vinylene. J. Am. Chem. Soc. *121*, 9852–9866.
20. Tew, G.N., Pralle, M.U., and Stupp, S.I. (2000). Supramolecular materials with electroactive chemical functions. Angew. Chem. Int. Ed. Engl. *39*, 517–521.
21. Pralle, M.U., Urayama, K., Tew, G.N., Neher, D., Wegner, G., and Stupp, S.I. (2000). Piezoelectricity in polar supramolecular materials. Angew. Chem. Int. Ed. Engl. *39*, 1486–1490.
22. Deb, S.K., Maddux, T.M., and Yu, L.P. (1997). A simple orthogonal approach to poly(phenylenevinylene) dendrimers. J. Am. Chem. Soc. *119*, 9079–9080.
23. Denkewalter, R.G., Kolc, J., and Lukasavage, W.J. September 1981. U.S. patent 4,289,872.
24. Meier, H., and Lehmann, M. (1998). Stilbenoid dendrimers. Angew. Chem. Int. Ed. Engl. *37*, 643–645.
25. Israelachvili, J.N. (1992). Intermolecular and Surface Forces (New York: Academic).
26. Chapman, T.M., Hillyer, G.L., Mahan, E.J., and Shaffer, K.A. (1994). Hydraamphiphiles - novel linear dendritic block copolymer surfactants. J. Am. Chem. Soc. *116*, 11195–11196.

27. Schenning, A.P.H.J., Elissen-Román, C., Weener, J.-W., Baars, M.W.P.L., Vandergaast, S.J., and Meijer, E.W. (1998). Amphiphilic dendrimers as building blocks in supramolecular assemblies. J. Am. Chem. Soc. *120*, 8199–8208.
28. Roman, C., Fischer, H.R., and Meijer, E.W. (1999). Microphase separation of diblock copolymers consisting of polystyrene and acid-functionalized poly(propylene imine) dendrimers. Macromolecules *32*, 5525–5531.
29. Cui, G.L., Xu, Y., Liu, M.Z., Ji, T., Chen, Y.M., and Li, Y.F. (1999). Highly ordered assemblies of dendritic molecules bearing multihydrophilic head groups. Macromol. Rapid Comm. *20*, 71–76.
30. Felder, D., Gallani, J.L., Guillon, D., Heinrich, B., Nicoud, J.F., and Nierengarten, J.F. (2000). Investigations of thin films with amphiphilic dendrimers bearing peripheral fullerene subunits. Angew. Chem. Int. Ed. Engl. *39*, 201–204.
31. Kung, H., Lee, C., Zhuang, Z., Kung, M., Hou, C., and Plossl, K. (2001). Novel stilbenes as probes for amyloid plaques. J. Am. Chem. Soc. *123*, 12740–12741.
32. Nitta, T., Arai, T., Takamatsu, H., Inatomi, Y., Murata, H., Iinuma, M., Tanaka, T., Ito, T., Asai, F., Ibrahim, I., et al. (2002). Antibacterial activity of extracts prepared from tropical and subtropical plants on methicillin-resistant *Staphylococcus aureus*. J. Health Sci. *48*, 273–276.
33. Pervaiz, S. (2003). Resveratrol: from grapevines to molecular biology. FASEB J. *17*, 1975–1985.
34. Nelson, J.C., Saven, J.G., Moore, J.S., and Wolynes, P.G. (1997). Solvophobically driven folding of nonbiological polymers. Science *277*, 1793–1796.
35. Bohn, P.W. (1993). Aspects of structure and energy transport in artificial molecular assemblies. Annu. Rev. Phys. Chem. *44*, 37–60.
36. Ohsaki, M., Okuda, T., Wada, A., Hirayama, T., Niidome, T., and Aoyagi, H. (2002). In vitro gene transfection using dendritic poly(L-lysine). Bioconjug. Chem. *13*, 510–517.
37. Wadie, J.S., and Dowdy, S.F. (2002). Protein transduction technology. Curr. Opin. Biotechnol. *13*, 52–56.
38. Wender, P.A., Mitchell, D.J., Pattabiraman, K., Pelkey, E.T., Steinman, L., and Rothbard, J.B. (2000). The design, synthesis, and evaluation of molecules that enable or enhance cellular uptake: peptoid molecular transporters. Proc. Natl. Acad. Sci. USA *97*, 13003–13008.